SAND93-2642C

CHARACTERIZATION OF POLYSILICON FILMS BY RAMAN SPECTROSCOPY AND TRANSMISSION ELECTRON MICROSCOPY: A COMPARATIVE STUDY*

(Proceedings of the 1993 Fall Meeting, Materials Research Society, Boston, MA, 11/29/93-12/3/93; Symposium K: Semiconductor Materials Processing)

CONF-931108--111

DAVID R. TALLANT**, THOMAS J. HEADLEY**, JOHN W. MEDERNACH** and FRANZ GEYLING***
**Sandia National Laboratories, Albuquerque, NM
***SEMATECH, Austin, TX.

ABSTRACT

Samples of chemically-vapor-deposited micrometer- and sub-micrometer-thick films of polysilicon were analyzed by transmission electron microscopy (TEM) in cross-section and by Raman spectroscopy with illumination at their surface. TEM and Raman spectroscopy both find varying amounts of polycrystalline and amorphous silicon in the wafers. Raman spectra obtained using blue, green and red excitation wavelengths to vary the Raman sampling depth are compared with TEM cross-sections of these films. Films showing crystalline columnar structures in their TEM micrographs have Raman spectra with a band near 497 cm^{-1} in addition to the dominant polycrystalline silicon band (521 cm^{-1}). The TEM micrographs of these films have numerous faulted regions and fringes indicative of nanometer-scale silicon structures, which are believed to correspond to the 497 cm^{-1} Raman band.

INTRODUCTION

Polysilicon films, which have microelectronic applications, are produced by chemical-vapor-deposition (CVD) using tube furnaces, plasmas and rotating disk reactors, among other techniques. The silicon deposited in this manner ranges from fully (poly)crystalline to amorphous, depending on the conditions in the reactor. It is necessary, then, to characterize the silicon present in the polysilicon films and correlate its structure with the reactor conditions in order to control the form of silicon produced. Two characterization techniques which have been successfully, but largely independently, used to characterize silicon structure are transmission electron microscopy (TEM) and Raman spectroscopy. The electron image produced by TEM (in either cross-section or "PLAN" view) provides visual indication of the grain size and shape of crystalline silicon domains and allows an estimate of the amount of crystalline versus amorphous structure. The spatial distribution of crystalline and amorphous regions is also apparent in TEM images. Raman spectroscopy is a light-scattering technique based on the inelastic interactions between incident photons and phonon modes in the material being illuminated. Inelastically scattered photons are shifted in energy by these interactions, and the resultant "Raman shift" corresponds to the phonon frequency (energy) involved in the interaction. For single crystal silicon or polycrystalline silicon with domains of 10nm or greater in size, the fundamental phonon mode is expressed as a narrow, symmetric Raman band occurring at a frequency shift (Raman shift) of about 521 cm^{-1} from the

MASTER

DISCLAIMER

Portions of this document may be illegible in electronic image products. Images are produced from the best available original document.

frequency of the incident photons [Pollack, 1985]. Tensile stress or domain sizes less than 10nm result in significant broadening and a decrease in the Raman shift of the fundamental band [Pollack, 1985]. The Raman band of amorphous silicon is broad and occurs in the 460-480cm^{-1} range [Pollack, 1985]. This paper presents the results of a joint TEM and Raman study of sub-micron-thick polysilicon films. Cross-sectional TEM images are compared to Raman spectra obtained with different effective depths of penetration by varying the frequency (wavelength) of the incident photons. Comparison of the TEM and Raman data provides insights into the structures of the polysilicon films not apparent from either set of data alone.

EXPERIMENTAL

The polysilicon films were deposited on 150mm diameter <100> silicon wafers on which had been grown 140nm of field oxide. The films were deposited in a rotating disk reactor using silane or disilane as the source gas under varying conditions of temperature and flow rate.

Samples were prepared in cross-section for TEM analysis. Cross-section pieces were wafered on a dicing saw, epoxied together, ground and polished to $\approx$125μm thickness, dimpled on the back side, ion-milled at a shallow angle to perforation and examined in a Phillips CM30 TEM at 300kV.

Raman spectra were obtained using a triple spectrograph with a charge-coupled detector (CCD). The spectrograph was operated at 6cm^{-1} resolution. Polysilicon film samples were analyzed as received with no further preparation. Film-side surfaces of the samples were illuminated with 100mW of the 457.9nm , 488.0nm and 514.5nm wavelengths from an argon-ion laser and the 647.1nm wavelength from a krypton-ion laser. The laser beam impinged the film surface at a 40° angle to it and was focused to an approximately 2mm by 0.1mm line. All Raman spectra in this paper are presented with a vertical intensity axis and a horizontal Raman shift axis.

EFFECTIVE RAMAN PENETRATION DEPTH

Visible light is strongly absorbed by elemental silicon, penetrating on the order of hundreds of nanometers. Absorption coefficients vary strongly with wavelength [Aspnes, 1983]. An estimate of the effective depth through which Raman signals are obtained is provided by Equation (1);

$$X_d = \text{func}(\varphi)/k_\upsilon[1 + \text{func}(\varphi)] \ (10^7 \text{nm/cm}) \qquad (1)$$

which was derived from Snell's Law of Refraction [Longhurst, 1967] and the absorption relation for radiation, $I = I_0\exp(-k_\upsilon x)$. $\text{func}(\varphi) = \cos(\sin^{-1}[\cos\varphi/n])$, where φ is the angle of the laser beam propagation with respect to the film surface, and n is the index of refraction of the film at frequency, υ. I_0 and I are the intensities of the light, respectively, at the surface and at depth x of the film, which has an absorption coefficient, k_υ (cm^{-1}) at frequency, υ (same value assumed for incident and inelastically scattered photons). X_d is the depth, in nm, from which inelastically scattered light, as measured at the film's surface, is 1/e the intensity of light from inelastic scatter events at the film's surface. Equation (1) takes into account attenuation of the incident laser photons by the film, the path of the laser beam in the film and attenuation of inelastically scattered photons during their propagation out of the film. Using Equation (1) with $\varphi = 40°$ and k_υ and n for crystalline silicon from Aspnes [1983], the effective penetration depths for the laser

wavelengths used in this study are shown in Table 1. Note that these penetration depths are estimates valid only for crystalline silicon. Absorption coefficients for amorphous silicon are not as well known but appear to be at least ten times as large as for crystalline silicon [Bosch, 1982]; penetration depths will be reduced proportionately in amorphous silicon. There is some experimental evidence (referred to later in this paper) that reflection or interference effects at the field oxide layer prevents penetration of light past the field oxide layer.

TABLE 1
Effective Raman Penetration Depth in Crystalline Silicon

Wavelength, nm	X_d (nm)
457.9	136
488.0	241
514.5	331
647.1	1473

RESULTS AND DISCUSSION

Figure 1 shows the TEM micrograph of a polysilicon film and the corresponding Raman spectra with excitation wavelengths as indicated. The light band at the bottom of the micrograph is the field oxide layer. Raman scatter from the field oxide was found to be of too low an intensity to contribute significantly to the Raman spectra presented in this paper, even in situations where the excitation wavelength is expected to penetrate to the field oxide layer. Effective Raman penetration depths (estimated for crystalline silicon - Table 1) for the excitation wavelengths are also indicated in the figure. The dark/light irregular features in the micrograph are regions of crystalline silicon. The featureless, smooth areas are interpreted as regions of amorphous silicon. The micrograph suggests that regions of mixed crystalline and amorphous silicon phases underlie a crystalline surface. Below a depth of 0.4μm, the silicon appears to be totally amorphous. The Raman spectra change as expected for increasing penetration depth with increasing excitation wavelength. For the shorter excitation wavelengths (457.9-514.5nm) the Raman spectra show a narrow band due to crystalline silicon (520cm^{-1}) and broader band of lower peak intensity due to amorphous silicon (483cm^{-1}), which increases slowly in relative intensity as the excitation wavelength (and penetration depth) increases. Even if the upper layers of the film were totally crystalline silicon, only the 647.1nm excitation wavelength would be expected to penetrate below the crystalline layers to the totally amorphous region. The Raman spectrum obtained with 647.1nm excitation shows a significantly increased relative intensity in the amorphous silicon band, corresponding to the totally amorphous silicon layer below 0.4μm in depth. The high absorptivity of the amorphous silicon region probably prevents significant penetration of even the 647.1nm wavelength through the totally amorphous region to the field oxide layer.

Figure 2 shows the TEM micrograph and corresponding Raman spectra of a polysilicon film with what appears from the micrograph to be a region of totally amorphous silicon overlying scattered silicon crystallites. With the relatively high absorptivity of amorphous silicon the actual penetration of the excitation wavelengths may be 10% of the effective penetration depths for crystalline silicon (as indicated in Table 1 and the figure). The 457.9nm excitation wavelength does not penetrate the totally amorphous layer, so that the 457.9nm-excited Raman spectrum shows only the amorphous silicon band (480cm^{-1}). The 647.1nm excitation wavelength is

expected to penetrate between 0.1 and 0.2μm in amorphous silicon (10% of the value in Table 1) and so has a low-intensity band near 521cm^{-1} indicative of the scattered silicon crystallites in addition to the dominant amorphous silicon band.

Figure 3 shows the TEM micrograph of a film with an apparently crystalline but columnar silicon structure throughout its depth. The associated Raman spectra show a dominant band due to crystalline silicon (521cm^{-1}) plus a low-intensity band peaking near 497cm^{-1}. The band near 497cm^{-1} corresponds to neither crystalline silicon nor amorphous silicon. The constancy of the intensity ratios of the 497 and 521cm^{-1} bands for 457.9 and 647.1nm excitation wavelengths suggests: one, that the species responsible for the 497cm^{-1} band is associated with the columnar structures and is in approximately constant concentration throughout the depth of the film; and two, that the 647.1nm excitation does not penetrate past the field oxide layer (possibly due to reflection or interference effects) to the substrate silicon. If the 647.1nm excitation significantly sampled the silicon substrate, the intensity of the crystalline silicon (521cm^{-1}) band should increase relative to the intensity of the 497cm^{-1} band.

An expanded image (see Figure 4) of the micrograph in Figure 3 shows numerous striations or fringes in the columnar silicon structures. These features are believed to be faults or dislocations on the nanometer scale. A micrograph of an annealed film prepared under similar conditions (Figure 5) does not show the columnar structures and dislocations, only relatively large crystalline regions. The Raman spectrum of the annealed film (Figure 5) lacks the 497cm^{-1} band and has a significantly narrowed band due to crystalline silicon. We conclude that the Raman band near 497cm^{-1} corresponds to the faulting present in the micrographs of the as-deposited film (Figures 3-5), which we believe to be nanometer-scale silicon structures, perhaps only a few unit cells in extent. Olego and Baumhart (1988) observed a similar Raman band at 490-500cm^{-1}, which they ascribed to surface layers of silicon that act as grain boundaries for crystalline silicon inclusions in an SiO$_2$ matrix.

SUMMARY

TEM micrographs and Raman spectra of polysilicon films provide confirmatory and complementary information for the identification of crystalline and amorphous phases and their spatial distribution. Dislocations or faulting in TEM micrographs of columnar structures in polysilicon films are correlated to a specific band at 497cm^{-1} in Raman spectra and identified as nanometer-scale silicon structures. Thus, comparison of TEM and Raman data provides insights not available from either set of data alone. More sophisticated modeling of the effective Raman penetration depth using accurate values for the absorption coefficient of amorphous as well as crystalline silicon should improve the correlation between TEM and Raman data.

REFERENCES

F. H. Pollack, Test and Measurement World, pp. 2-10 (May, 1985)

D. E. Aspnes and A. A. Studna, Phys. Rev. B, **27**(2), 985-1009 (1983).

M. A. Bosch and R. A. Lemons, Appl. Phys. Lett. **40**(2), 166-168 (1982).

D. J. Olego and H. Baumgart, J. Appl. Phys. **63**(8), 2669-2673 (1988).

R. S. Longhurst, in <u>Geometrical and Physical Optics,</u> 2nd Ed., (Longman Group Ltd, London, 1967). p. 5.
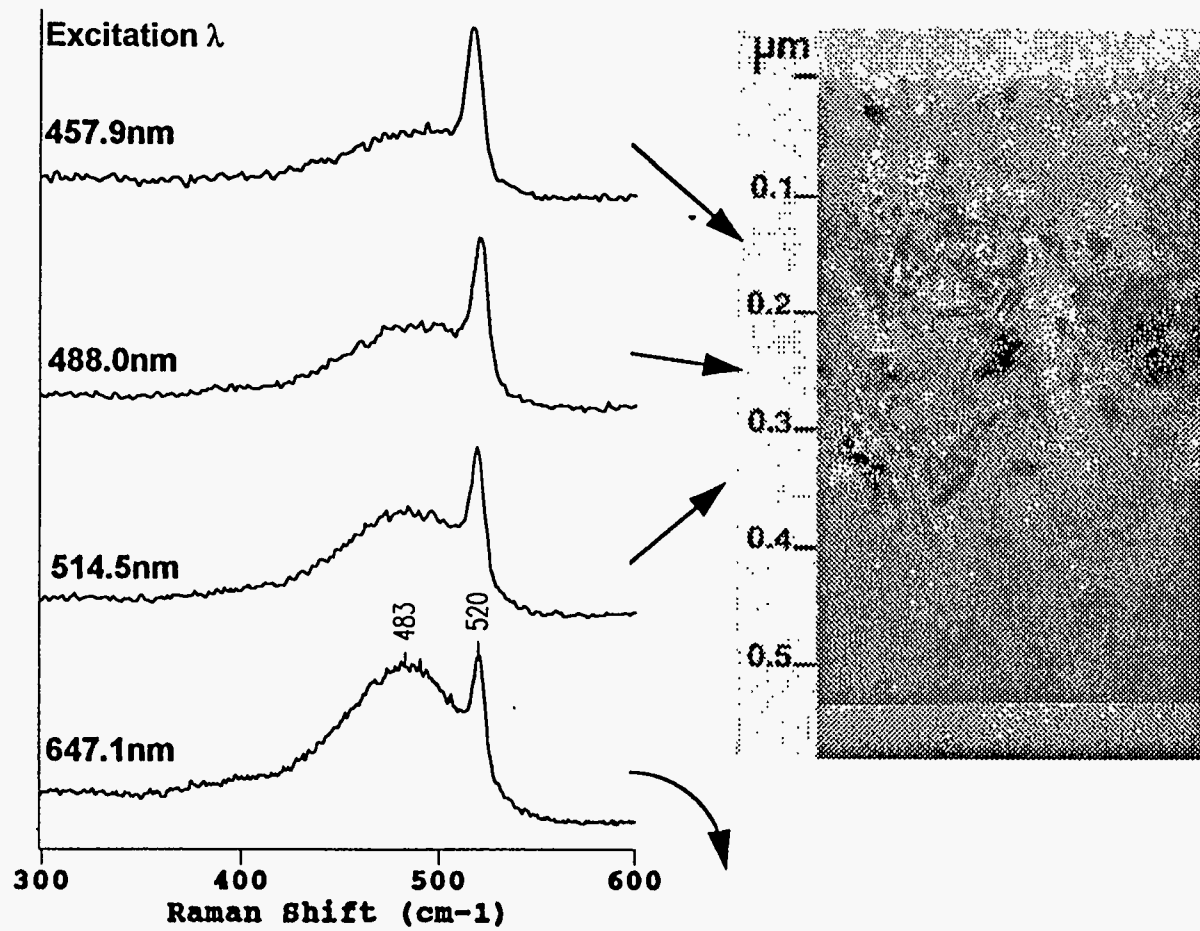
DISCLAIMER

Figure 1. TEM micrograph and Raman spectra of a polysilicon film. Arrows point to the effective penetration depth of the excitation wavelength in crystalline silicon.
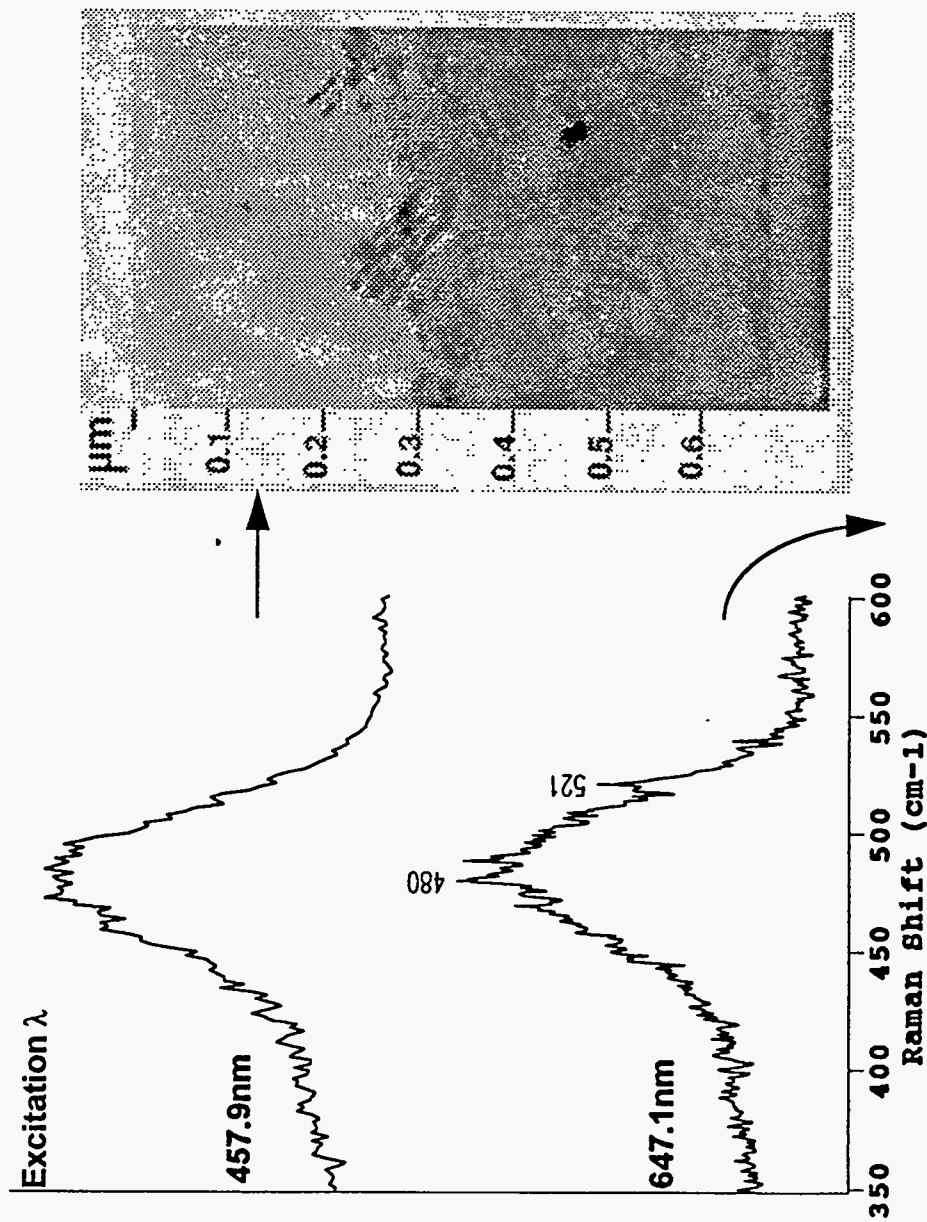
Figure 2. TEM micrograph and Raman spectra of a polysilicon film . Arrows point to the effective penetration depth of the excitation wavelength in crystalline silicon.
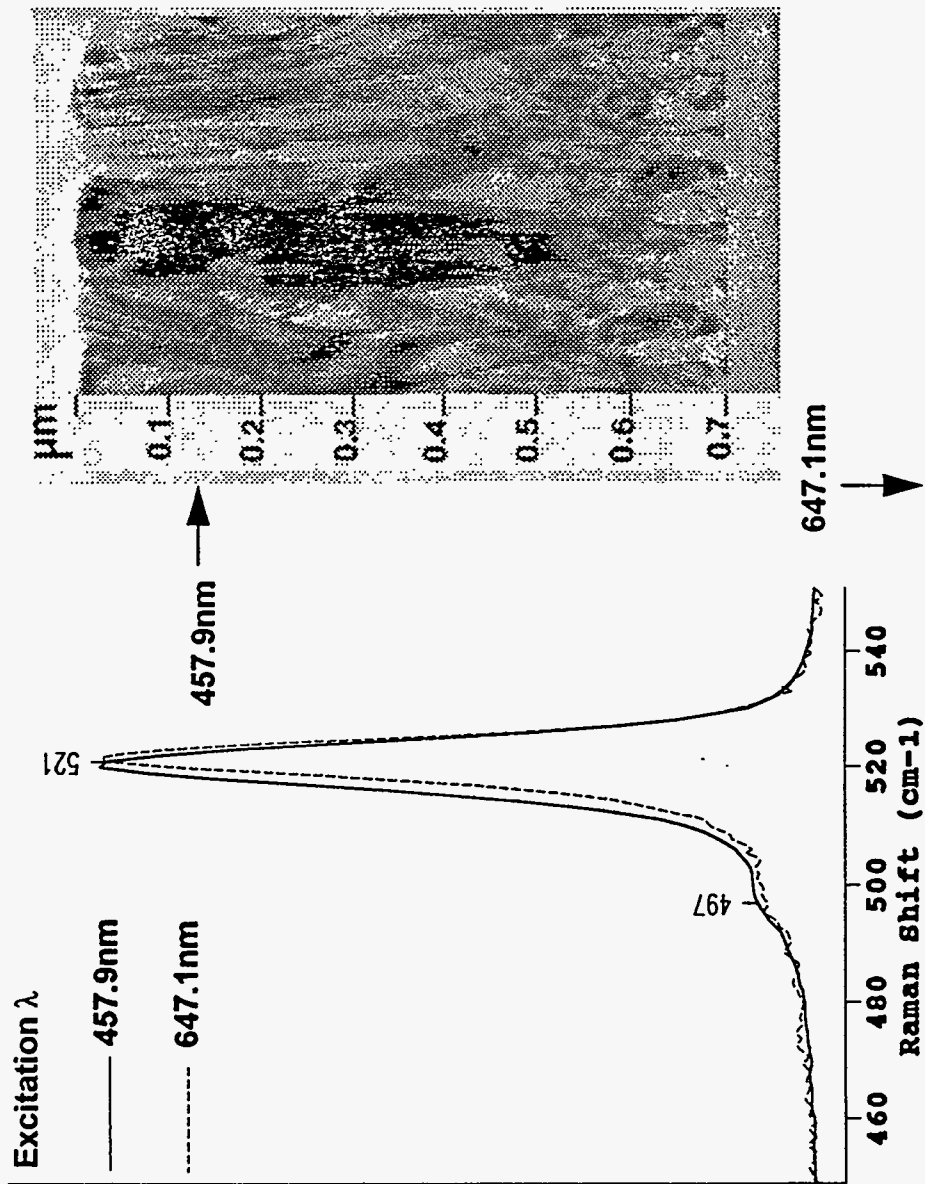
Figure 3. TEM micrograph and Raman spectra of a polysilicon film. Arrows point to the effective penetration depth of the excitation wavelength in crystalline silicon.
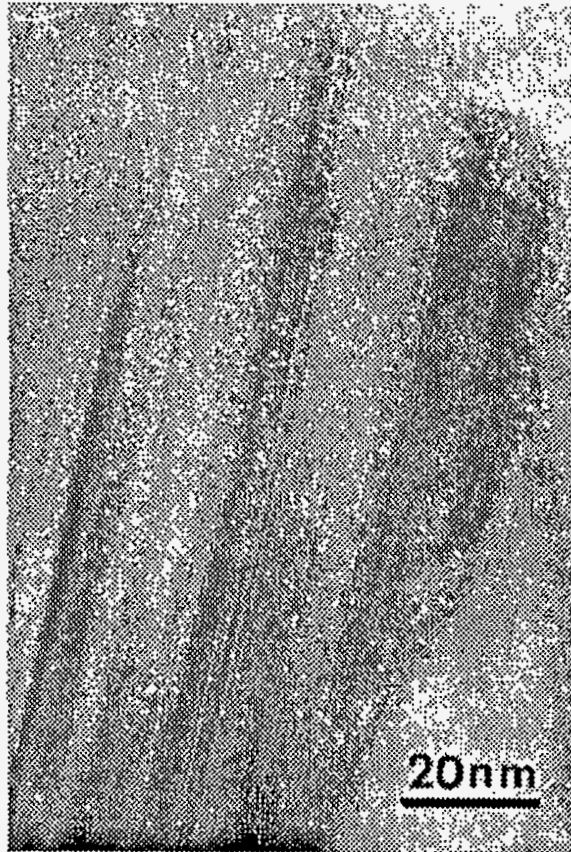
Figure 4. Expanded TEM micrograph of
the columnar structures in the polysilicon
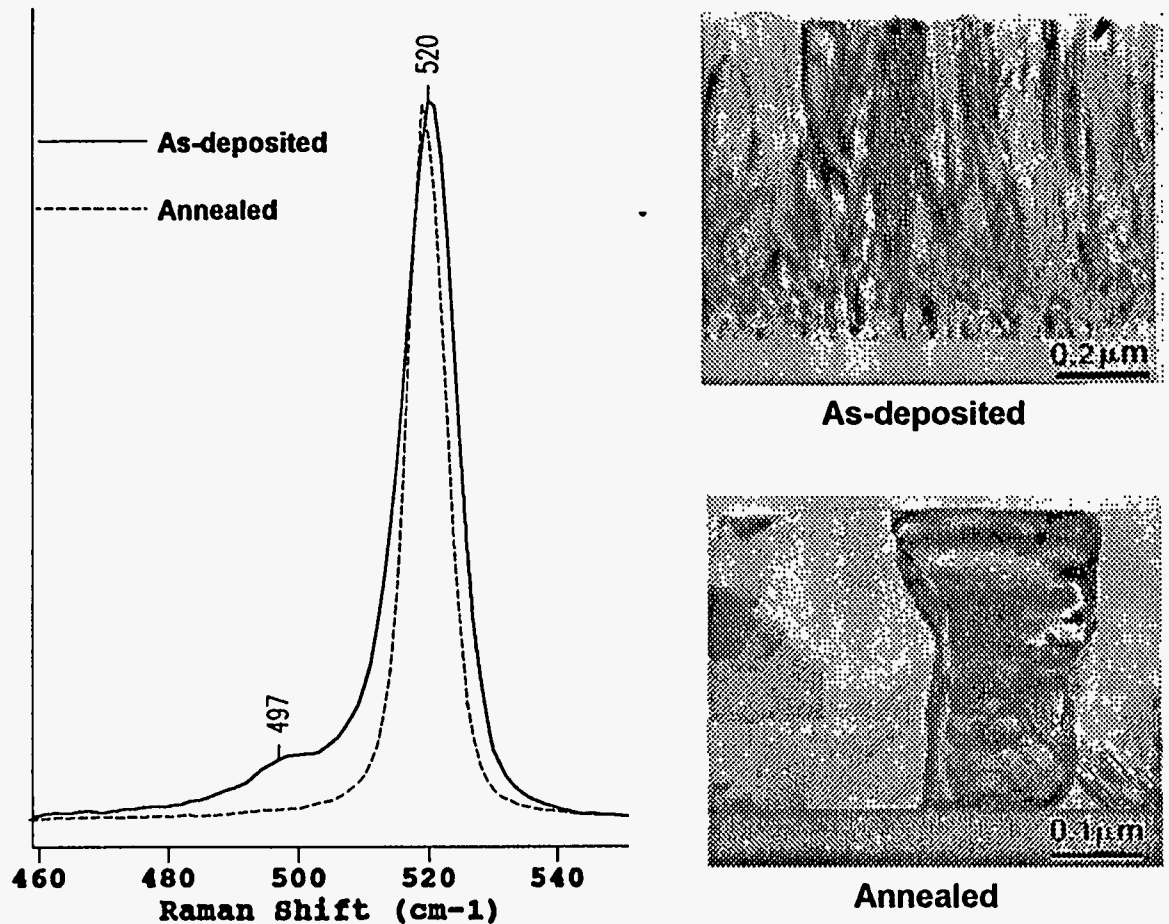film also shown in Figure 3.

Figure 5. TEM micrographs and Raman spectra of the as-deposited polysilicon film with a columnar structure (see Figures 3 and 4) and an annealed film.